Lateral-Torsional Buckling of Structural Glass Beams. Experimental, Theoretical and Numerical Analysis

Ondřej Pešek and Jindřich J. Melcher
Institute of Metal and Timber Structures, Brno University of Technology, Brno, Czech Republic
Email: pesek.o@fce.vutbr.cz, melcher.j@fce.vutbr.cz

***Abstract*—This paper deals with experimental research of stability behaviour of laminated structural glass beams. The purpose of the research is the evaluation of lateral-torsional buckling resistance and actual behaviour of the beams due to absence of standards for design of glass load-bearing structures. The experimental research follows the previous one focusing on measuring of initial geometrical imperfections of glass members and experimental evaluation of flexural buckling resistance of structural glass columns. Within the frame of the research 9 specimens were tested. Experiment results were compared with analytical analysis and numerical analysis based on finite element method using initial imperfections resulted from Southwell's plot. The goal of the research is to develop buckling curve parameters to simple calculation of buckling resistance.**

***Index Terms*—lateral-torsional buckling, laminated glass, structural glass, finite element method, second order theory, buckling curves**

I. Introduction

Glass members and structures are specific for their high slenderness. For this reason it is necessary to take into account stability problems within static designing. Fig. 1 shows glass fins supporting glass fa çade (Funda ção Champalimaud in Lisbon, Portugal). Glass fin acts as beam (with span 12 m) due to wind load.

Design models developed for standard structural materials such as steel and timber cannot be directly used for design of glass structures because of some specific aspects of the glass (brittle fracture behaviour, time and temperature dependency of laminated glass etc.). Actually European design standards (Eurocodes) are in processing, designers may use draft versions of future final codes - prEN 16612 Glass in building – Determination of the load resistance of glass panes by calculation and testing or prEN 13474-1 Glass in building – Design of glass panes – Part 1: General basis of design. Feldmann et al. [1] give the most actual design guidance including overview of actual European research in structural glass.

Figure 1. Glass fins supporting glass fa çade.

Haldimann [2], [3] offer deep knowledge of structural glass fracture strength, analytical and numerical modeling and testing as a base for static design. Belis et al. [4] deal with structural glass elements initial geometrical imperfections that have influence on element structural resistance. Amadio and Bedon [5], [6] and Belis [7] describe results of their research on stability problems of glass columns, beams and beam-columns.

This study follows previous author's researches on structural glass member's geometrical imperfections [8] (in press), load bearing resistance and behaviour of glass

Manuscript received October 9, 2017; revised October 16, 2018.

doi: 10.18178/ijscer.7.4.323-330

columns [9] and structural behaviour of laminated glass beams [10] and beams-columns [11].

Lateral-torsional buckling is loss of stability of bended member subjected to a rigid axis – see Fig. 2.

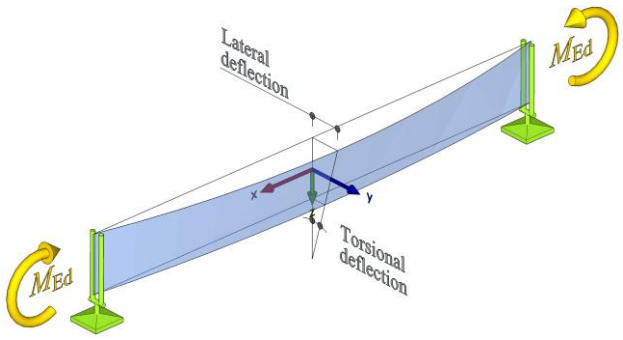

Figure 2. Lateral and torsional deflections of a beam subjected to the lateral-torsional buckling.

In the case of laminated glass member it is necessary to take into account an actual behaviour of the laminated cross section because of additional degree of freedom for bending and torsion of laminated glass – see Fig. 3.

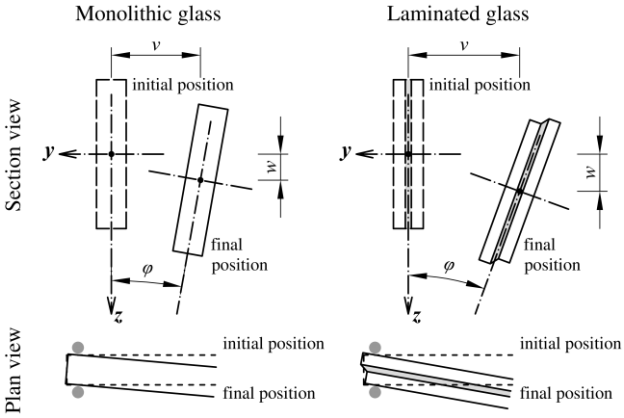

Figure 3. Additional deformation due to glass laminating.

Structural behaviour of beam made of laminated structural glass depends on interlayer material – interlayer bonding glass panes together and ensure interaction of them. Interlayer materials (polyvinyl butyral, Ionoplast, ethylene vinyl acetate, resin) are viscous-elastic materials – their material characteristic strongly depends on temperature and loading time. These aspects have to be taking into account in laminated glass analysis.

Fig. 4 shows behaviour of beam bended on strong axis, the behaviour is strongly nonlinear, deflections decreasing faster than loading force (bending moment). This nonlinearity is caused by imperfections: geometrical, material and structural. With bigger initial imperfections the nonlinearity is stronger from beginning of beam loading. *P*-Δ curve converge to the elastic critical moment M_{cr} that is for perfect beam without imperfections.

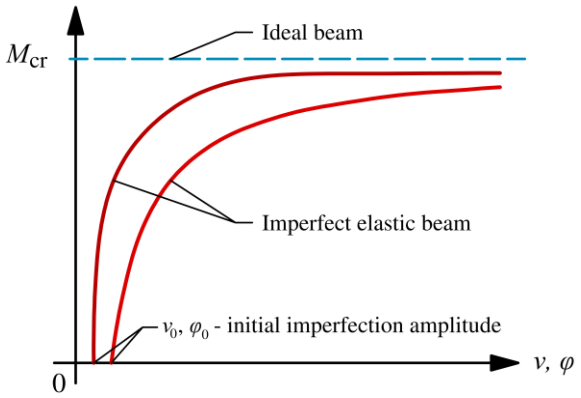

Figure 4. Load-deflection curve.

II. Experimental Analysis

Experiments were carried out in Institute of Metal and Timber Structures laboratories.

A. Specimens

Within the frame of the research 9 specimens were tested. All of them were of the same geometry (length 2400 mm, width 280 mm) and same composition (laminated double glass made of annealed glass panes bonded together by PVB foil 0.76 mm thick). Overall thicknesses of specimens were 12, 16 or 20 mm. The specimens are listed in Table I. 3 pieces of each type were tested.

Specimen geometry was chosen so that thin-walled (thin-walled in terms of structural mechanics, not steel structures) rod condition was fulfilled. Vlasov [12] defined a thin-walled rods by condition $L : b : t = 100 : 10 : 1$, where L is length of the rod, b is characteristic dimension of the cross section, and t is the wall thickness of the cross section.

TABLE I. List of Tested Specimens

Designation	Description	Length Width	Glass th. Foil th.
VG 66.2	Laminated double glass made of annealed glass using EVASAFE foil	2400 280 [mm]	6+6 0.76 [mm]
VG 88.2	Laminated double glass made of annealed glass using EVASAFE foil	2400 280 [mm]	8+8 0.76 [mm]
VG 1010.2	Laminated double glass made of annealed glass using EVASAFE foil	2400 280 [mm]	10+10 0.76 [mm]

B. Test Set-up

The specimen was placed in a steel frame consisting of steel girder and columns. Loading force was generated by electrically operated hydraulic press. Test set-up is plotted in Fig. 5. Fork support conditions were ensured by steel coulters fitted on both ends of specimen. Coulter was equipped with gusset plate consisting hole for pin – see Fig. 6 (a). Timber pads situated between steel parts and the glass specimen avoided direct contact of the steel and the glass which may cause a failure by local stress concentrations in contacts – see detail in Fig. 6 (b).

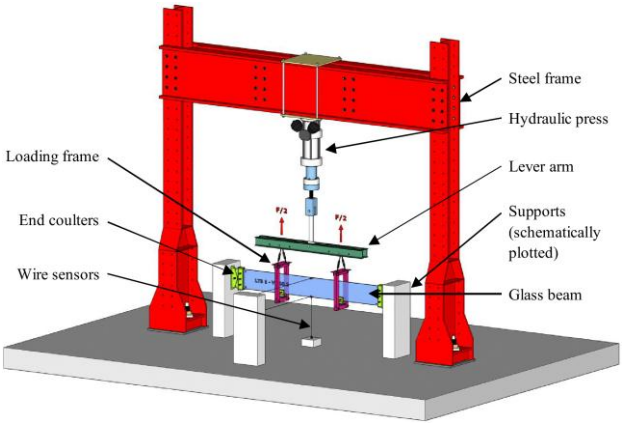

Figure 5. Test set-up.

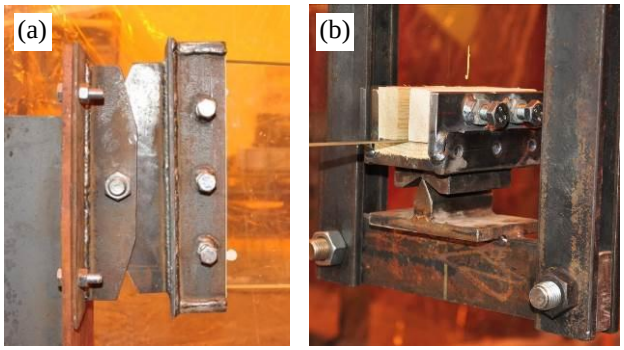

Figure 6. Detail of support and load introduction point.

Specimen was loaded by two, symmetrically to the mid-span situated, concentrated loads – specimen was subjected by four point bending. Loading force was ensured by one electro hydraulic press and was introduced into specimen by balance arm and loading frames (Fig. 7) into two points approximately in third of the length of the beam. Supporting blocks illustrated in figure are plotted only schematically.

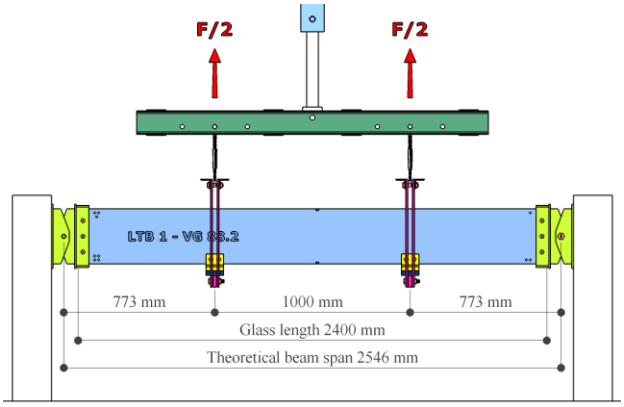

Figure 7. Note how the caption is centered in the column.

Loading force F, vertical deflection w_3 and horizontal (lateral) deflections (at bottom edge v_2 and at upper edge v_1) at mid-span were measured within testing using force transducer and wire sensors respectively. Normal stresses at extreme fibers at concave and convex side of beam at mid-span were measured using strain-gauges T4, T5, T6, T7 glued to sanded glass. Scheme of measuring devices is plotted in Fig. 8.

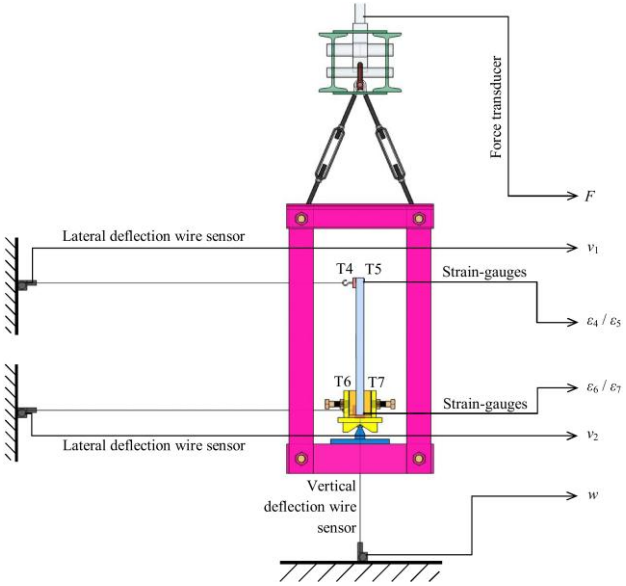

Figure 8. Measured variables – mid span cross section.

Tested specimens were loaded by static force up to failure of specimen. Loading rate was determined by the press cylinder pull (0.08 mm.s^{-1} for VG 1010.2; 0.04 mm.s^{-1} for VG 88.2; 0.02 mm.s^{-1} for VG 66.2).

C. *Failure Mechanism*

All of the specimens were destroyed by brittle fracture. In six cases from nine specimens, the point of primary failure origin was situated in the point of right force introduction or close to this point. It may indicate that there was some asymmetry in test set up geometry. As example fracture pattern of specimens LTB1, LTB4 and LTB9 are plotted in Fig. 9.

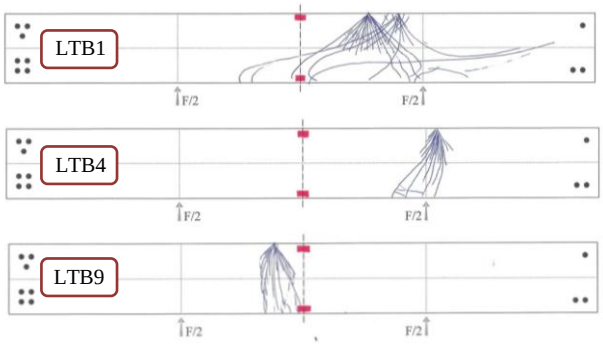

Figure 9. Measured variables – mid span cross section.

D. *Results*

Actual behaviour of laminated glass beams is described by load - deflection curves plotted in Fig. 10: a) load-lateral deflection, b) load-normal stress and c) load-angle of torsion. Lateral deflections are plotted for cross section centroid; these values were calculated from measured points on bottom and upper edges of glass cross section assuming rigid cross section. Influence of second order theory is good visible for specimens made of VG 66.2 with thickness of glass 12 mm; for specimens made of VG 1010.2 with thickness of glass 20 mm this influence is negligible.

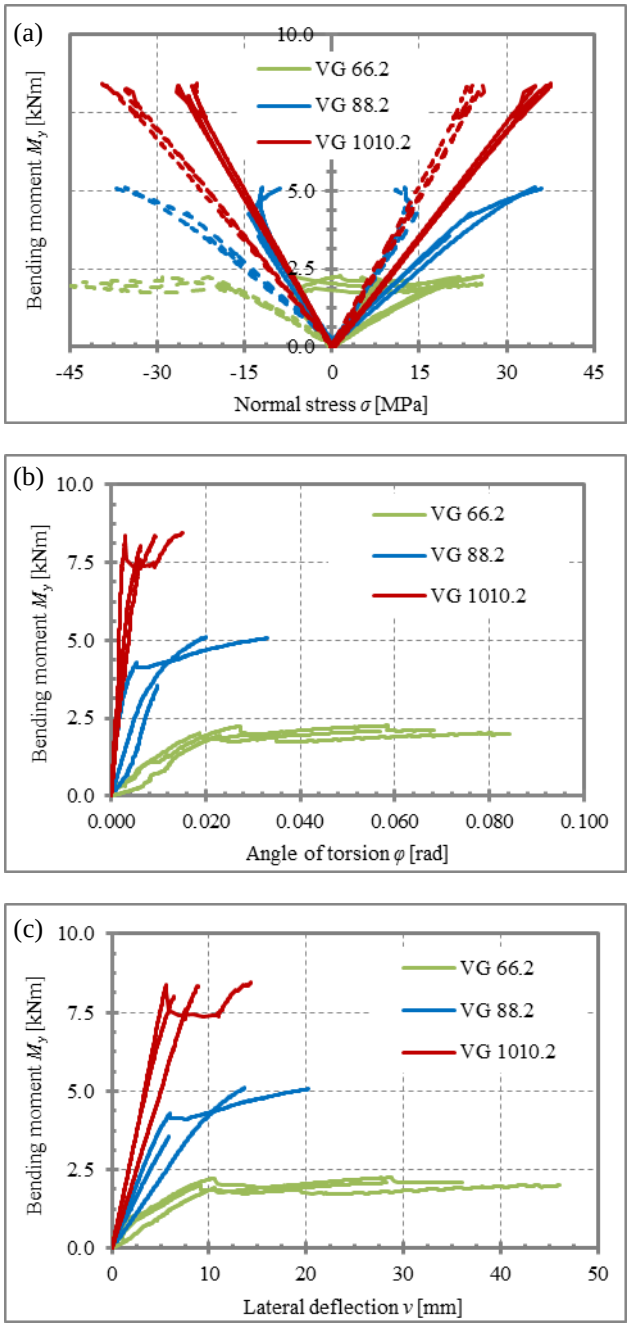

Figure 10.Test results: load – deflection curves. a) normal stresses; b) angle of torsion; c) lateral deflection.

The maximum bending moment, normal tensional stress and deflections at the time of specimen's failure are listed in Table II. The maximum achieved bending moment (bending resistance) in the groups of three same specimens are similar except specimen LTB6 that collapsed under significantly lower load than other two.

Achieved maximum bending resistances were statistically evaluated according to the EN 1990, appendix D [13]. Mean values, characteristic values and design values were calculated assuming normal distribution – see Fig. 11.

TABLE II. TEST RESULTS

Specimen	v_{max}	w_{max}	φ_{max}	M_{max}	σ_{max+}	t_{test}
	[mm]	[mm]	[rad]	[kNm]	[MPa]	[s]
LTB1	8.87	10.58	0.0093	8.36	37.58	645
LTB2	6.39	7.13	0.0062	8.02	35.15	363
LTB3	14.26	11.11	0.0151	8.45	37.66	352
LTB4	13.68	5.95	0.0200	5.12	34.85	432
LTB5	20.21	8.57	0.0330	5.07	36.03	461
LTB6	5.87	5.73	0.0098	3.55	20.13	327
LTB7	36.09	16.13	0.0682	2.26	25.82	865
LTB8	46.15	18.79	0.0844	2.02	21.53	1076
LTB9	28.27	12.25	0.0570	2.24	21.91	817

Due to one defective specimen (LTB6) made of VG 88.2 variation coefficient COV is relatively high in comparison with two other. This fact result in lower characteristic and design values than for thicker specimens VG 66.2.

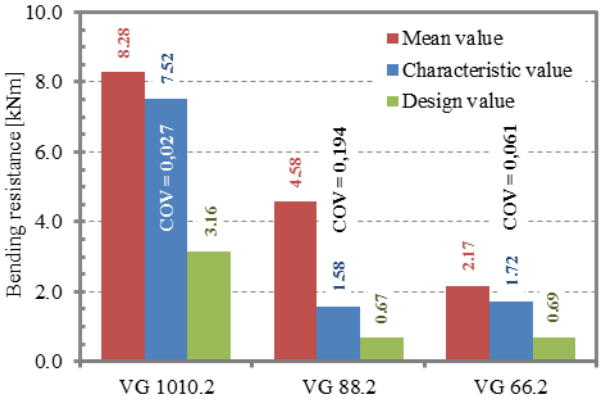

Figure 11. Statistical evaluation of experimental analysis.

E. *Equivalent Imperfections*

Equivalent flexural critical moments $M_{cr,exp}$ and initial geometrical imperfections (lateral deflection and torsional deflection) were calculated (if possible) using Southwell's method [14] – see Fig. 12.

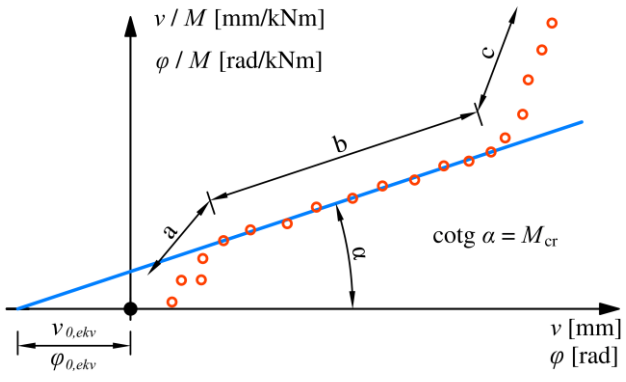

Southwell plot.

Figure 12. Resulting values are listed in Table III.

TABLE III. SOUTHWELL'S PLOT RESULTS

Specimen	Mcr,exp			Equivalent initial geometrical imperfections		
	Lateral deflection	Torsional deflection	average	Lateral deflection	Torsional deflection	
	[kNm]			[mm]	[rad]	[°]
LTB1	unable to determine	10.938	10.938	unable to determine	0.0030	0.173
LTB2	10.934	11.081	11.008	2.409	0.0024	0.138
LTB3	11.736	11.304	11.520	5.582	0.0049	0.279
LTB4	5.546	5.724	5.635	1.437	0.0027	0.156
LTB5	5.268	5.269	5.268	1.998	0.0023	0.133
LTB6	5.397	unable to determine	5.397	6.506	unable to determine	unable to determine
LTB7	2.652	2.510	2.581	6.770	0.0101	0.577
LTB8	2.303	2.191	2.247	9.836	0.0137	0.784
LTB9	2.376	2.335	2.355	5.753	0.0106	0.606

III. THEORETICAL ANALYSIS

Kasper [15] published equations to calculate torsional deformation $\varphi(x)$ (1) and lateral deflection $v(x)$ (2) of imperfect bended beam according to the second order theory. These equations are valid for sinusoidal initial imperfections (initial lateral deformation v_0 and initial torsional deformation φ_0) shape and fork boundary conditions.

$$\varphi(x)=\frac{\varphi_0\left(\frac{c_1^2\cdot M_y^2}{E\cdot I_z}-c_2\cdot\left(\frac{\pi}{L}\right)^2\cdot M_y\cdot z_g\right)+c_1\cdot\left(\frac{\pi}{L}\right)^2\cdot M_y\cdot v_0}{G\cdot I_t\cdot\left(\frac{\pi}{L}\right)^2-\frac{c_1^2\cdot M_y^2}{E\cdot I_z}+c_2\cdot\left(\frac{\pi}{L}\right)^2\cdot M_y\cdot z_g}\cdot\cos\left(\frac{\pi}{L}\cdot x\right) \quad (1)$$

$$v(x)=\frac{c_1\cdot\frac{G\cdot I_t}{E\cdot I_z}\cdot M_y\cdot\varphi_0+c_1^2\cdot\frac{M_y^2}{E\cdot I_z}\cdot v_0}{G\cdot I_t\cdot\left(\frac{\pi}{L}\right)^2-\frac{c_1^2\cdot M_y^2}{E\cdot I_z}+c_2\cdot\left(\frac{\pi}{L}\right)^2\cdot M_y\cdot z_g}\cdot\cos\left(\frac{\pi}{L}\cdot x\right) \quad (2)$$

In equations there E is Young's modulus of glass, G is glass shear modulus, M_y is bending moment to strong axis, L is beam span, I_z is moment of inertia to weak axis (in the case of laminated glass effective moment $I_{z,eff}$ is used), I_t is St. Venant torsion constant (in the case of laminated glass effective value $I_{t,eff}$ is used), z_g is distance from shear center to loading point (positive or negative value) and x is distance of point of interest from mid-span. Constants c_1 and c_2 (3) depends on type of load

$$c_1=\frac{1}{C_1};\quad c_2=2\frac{C_2}{C_1} \quad (3)$$

where Constants C_1 and C_2 are constants according to national annexes of EN 1993-1-1 [16].

According to (4) it is possible to simplify calculate normal stresses σ_x in each point on cross section of bended beam (bimoment is neglected). W_y and W_z are section modulus on strong axis and weak axis respectively.

$$\sigma_x\approx\pm\frac{M_y}{W_y}\pm\frac{M_z}{W_{z,eff}} \quad (4)$$

Using (1), (2) and (4) it is possible to find load (bending moment) that cause normal stress σ_{+max} that achieve tensile strength of glass σ_{Rk}, this moment is buckling resistance $M_{b,Rk}$ – equation (5)

$$\sigma_{+max}=+\frac{M_y}{W_y}+\frac{M_z}{W_{z,eff}}=\sigma_{Rk}\rightarrow M_{b,Rk} \quad (5)$$

Fig. 13 shows dependency of normal stresses calculated according (4) on load and point of lateral-torsional buckling resistance for initial geometrical imperfections $v_0 = L/200$ and $\varphi_0 = 0$.

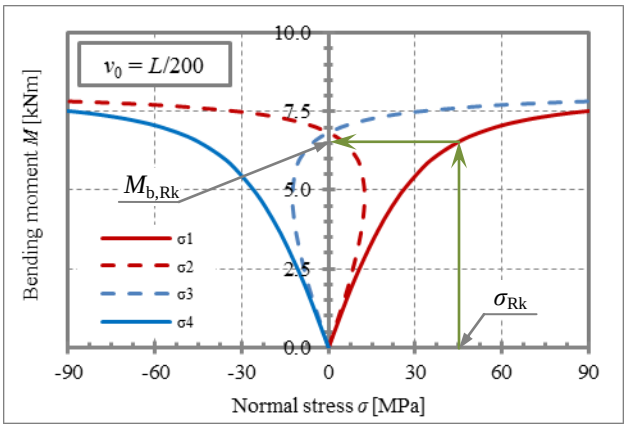

Figure 13. Theoretical analysis: stress-load dependency.

IV. NUMERICAL ANALYSIS

Numerical analysis was carried out in ANSYS software (mechanical APDL) [17] based on finite element method. Only laminated glass beam was modelled, The length of beam was same as theoretical beam span at experiments. Laminated glass was modelled using planar and spatial finite elements. Interlayer was meshed by bricks SOLID 185, thickness 0.75 mm was divided on four elements, and planar dimensions of elements were 20 mm. Glass panes were modelled by planar elements

SHELL 181 large 20 mm × 20 mm. Because of true position of glass panes centroid offset function was used.

Boundary conditions (both load and support) were modelled by definition of nodes displacement.

Linear stability analysis gives eigenvalues and eigenshapes. The first eigenshape is plotted in Fig. 14.

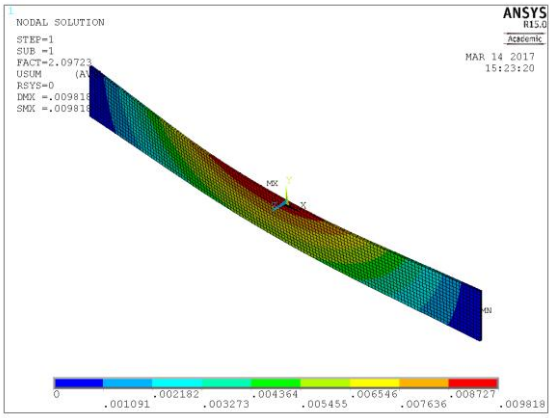

Figure 14. Linear stability analysis – first eigenshape.

Further step was to change geometry according to first eigenshape with imperfection amplitude of $L/300$ and $L/200$ that are approximately equal to maximum overall bow deformation 3 mm/m and 5 mm/m defined by production standards [18], [19].

Then GNIA (geometrically non-linear elastic analysis with imperfections) was carried out. Load forces were applied in 100 substeps, so that final load (last substep) caused bending moment equal to elastic critical moment for first eigenshape.

Dependency of normal stresses and deflections on applied bending moment were observed within the simulation. In Fig. 15 stresses-load curves ale plotted.

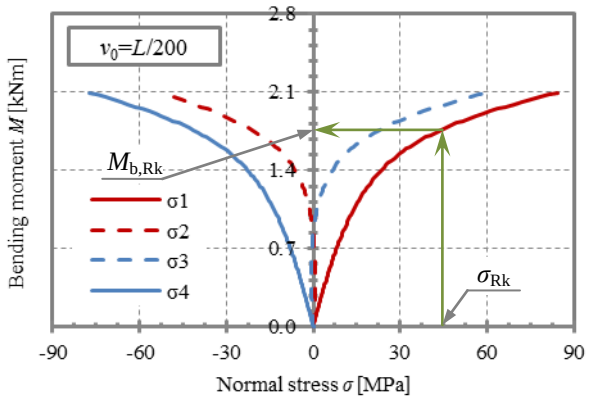

Figure 15.Numerical analysis: stress-load dependency.

The avaluation of numerical analysis was the same principle (6) like analytical analysis – the load caused normal stress that achieve glass strength was taken as lateral-torsional buckling strength.

$$\sigma_{+\max} = \sigma_{Rk} \rightarrow M_{b,Rk} \tag{6}$$

Fig. 16 shows normal stress distribution on convex surface of bended beam with imperfections.

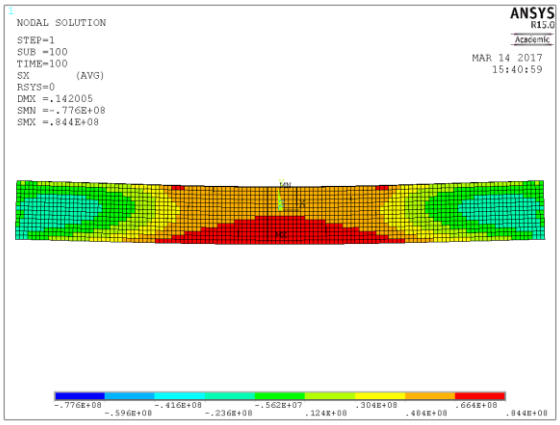

Figure 16. Numerical analysis: normal stress distribution.

V. Discussion

Results of experimental analysis were compared with analytical results and numerical modeling results. Fig. 17 shows relatively good agreement of calculated lateral deflections with measured within experiment for specimen LTB8 made of VG 66.2.

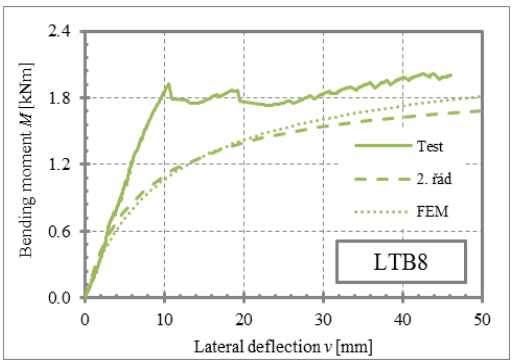

Figure 17. Result comparison: lateral deflection.

The same comparison is showed for normall stresses in Fig. 18. Finite element analysis gives much lower stresses for loads near critical moment than analytical analysis, but for low loads the the agreement is better.

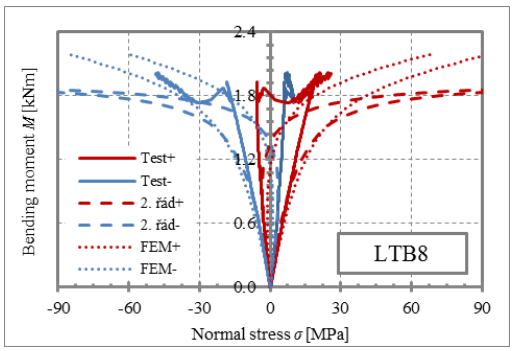

Figure 18. Result comparison: normal stress.

Interest comparison givs Fig. 19 where elastic critical moments M_{cr} are plotted for all types of simulation. Values from theoretical and numerical analysis are almost the same but they are much lower than actual values taken from experiments using Southwell's method. This is

caused by different boundary conditions within the tests (there were not exact fork conditions).

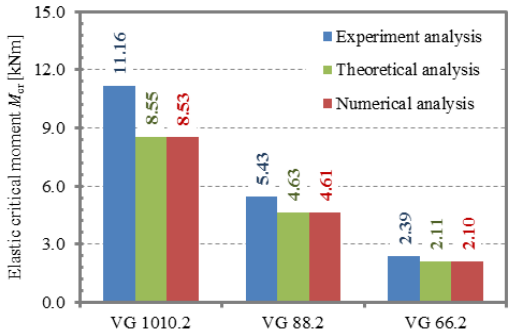

Figure 19. Result comparison: elastic critical moment.

Bending resistances given by three approaches are plotted in Fig. 20 and listed in Table IV. Values presented in Fig. 20 are mean values (average of three specimens in each approach). In this case for theoretical and numerical analysis equivalent geometrical initial imperfections from Southwell's method were used. Values listed in Tab. IV are characteristic and design values calculated according EN 1990 [13].

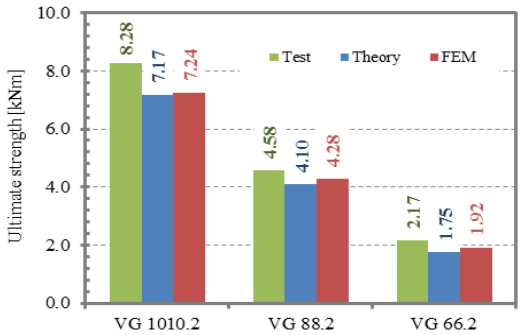

Figure 20. Result comparison: bending resistance.

Numerical and theoretical approach gives very similar results in all cases. In the case of mean values are lower than given from tests. The big difference between tests and theoretical and numerical analysis is in characteristic and design values for glass VG 88.2 but this phenomenon is caused by one defective specimen in combination with low number of specimens.

TABLE IV. RESULTS COMPARISON

Value	Glass	Method		
		Test	Theory	FEM
Mean	VG 1010.2	8.28	7.17	7.24
	VG 88.2	4.58	4.10	4.28
	VG 66.2	2.17	1.75	1.92
Characteristic	VG 1010.2	7.52	6.90	6.36
	VG 88.2	1.58	3.93	3.79
	VG 66.2	1.72	1.82	1.88
Design	VG 1010.2	3.16	2.76	2.54
	VG 88.2	0.67	1.57	1.52
	VG 66.2	0.69	0.73	0.75

The whole previous methods serve as a base for buckling curves approach, that will be use in further eurocode on design of glass structures. This research leads to develop buckling curves parameters α_{imp} and α_0 that describe the curve shape and gives a reduction factor χ_{LT} and lateral torsional buckling resistance $M_{b,Rd}$.

Amadio and Bedon [5] offer values α_{imp} = 0,26 and α_0 = 0,20. Haldimann [3] recomended use EC3 [16] curve c (α_{imp} = 0,49 and α_0 = 0,20) for design of stell rods. These curves are plotted in Fig. 21 and tests results are plotted by different marks for each type of specimens. Reduction factors given from tests $\chi_{LT,test}$ are calculated according (7), where $M_{ult,test}$ is maximal achieved bending moment and M_{Rk} is simple bending resistance (effective section modulus multiplied by tensile glass strength).

$$\chi_{LT,test} = \frac{M_{ult,test}}{M_{Rk}} \quad (7)$$

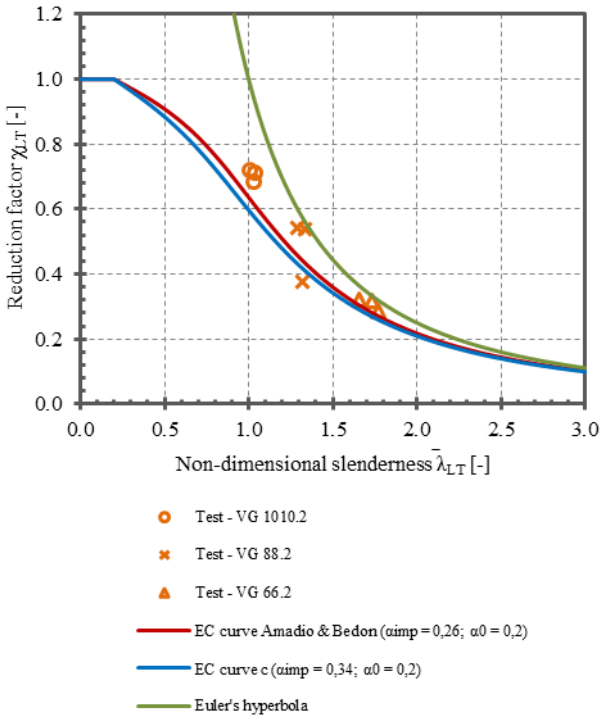

Figure 21. Reduction factor: test results and buckling curves.

VI. CONCLUSIONS

In the frame of experimental analysis 9 specimens were tested on lateral-torsional buckling. Results were statistically evaluated and they show strong dependency of ultimate strength on glass thickness. On the base of test analytical and numerical analysis were carried out so that initial geometrical imperfections were taken from test's Southwell's plot. Results of analytical solution and numerical solution are close to the tests one.

Reduction factors given from tests evaluation are higher than reduction factors given by using buckling curves approach – buckling curves approach is on the safe side for all articles published to this time.

Next step of research could be on different boundary conditions – both load and support. To give reliably buckling curve parameters, it is necessary to do more tests with different parameters.

This research together with the research on compressed members is a base for next research on lateral-torsional buckling and flexural buckling interaction (structural glass beam – columns behaviour).

ACKNOWLEDGMENT

This paper has been elaborated within the support of the Projects of Czech Ministry of Education, Youth and Sports: No FAST-S-17-4655.

REFERENCES

[1] M. Feldmann, R. Kasper et al., *Guidance for European Structural Design of Glass Components Support to the implementation, harmonization and further development of the Eurocodes*, Report EUR 26439 EN. Luxembourgh: Publications Office of the European Union, 2014, doi: 10.2788/5523.

[2] M. Haldimann, *Fracture Strength of Structural Glass Elements. Analytical and Numerical Modelling, Testing and Design*, Saarbrücken: Südwestdeutscher Verlag für Hochschulschriften, 2009.

[3] M. Haldimann, A. Luible and M. Overend, *Structural Use of Glass*, Zurich: ETH Zurich, 2008.

[4] J. Belis, B. Mocibob, A. Luible, and M. Vandebroek, "On the size and shape of initial out-of-plane curvatures in structural glass components," *Construction and Building Materials*, vol. 25, pp. 2700–2712, 2011.

[5] C. Amadio and Ch. Bedon, "Standardized buckling curves for the verification of glass columns, beams and panels," presented at the XXVII ATIV Conference, Parma, Italy, November 15-16, 2012.

[6] Ch. Bedon and C. Amadio, "Flexural-torsional buckling: Experimental analysis of laminated glass elements," *Engineering structures*, vol. 73, pp. 85-99, 2014.

[7] J. Belis, Ch. Bedon, Ch. Louter, C. Amadio and R. van Impe, "Flexural-torsional buckling: Experimental analysis of laminated glass elements," *Engineering structures*, vol. 51, pp. 295–305, 2013.

[8] O. Pešek and J. Melcher, "Shape and Size of Initial Geometrical Imperfections of Structural Glass Members," *Transactions of the VŠB – Technical University of Ostrava, Civil Engineering Series*, vol. 18, 2017.

[9] O. Pešek, J. Melcher and M. Horáček, "Experimental Verification of the Buckling Strength of Strucutral Glass Columns," *Procedia Engineering*, vol. 161, pp. 556–562, 2016, doi:10.1016/j.proeng.2016.08.691.

[10] O. Pešek and J. Melcher, "Lateral-Torsional Buckling of Laminated Structural Glass Beams. Experimental Study," *Procedia Engineering*, vol. 190, pp. 70–77, 2017, doi: 10.1016/j.proeng.2017.05.309.

[11] O. Pešek, J. Melcher and I Balázs, "Experimental Verification of the Structural Glass Beam-Columns Strength," *IOP Conference Series: Material Science and Engineering*, vol. 245, 2017, doi: 10.1088/1757-899X/245/3/032068.

[12] V. Z. Vlasov, *Thin-Walled Elastic Bars*, Prague, Czechoslovakia: State technical literature publishing, 1962.

[13] EN 1990. Eurocode: Basis of structural design. Brussels: European Committee for Standardization, 2011.

[14] V. Březina, *Buckling Load Capacity of Metal Rods and Beams*, Prague, Czechoslovakia: Czechoslovak Academy of Science, 1962.

[15] R. Kasper, „Tragverhalten von Glasträgern," Ph.D. dissertation, Schriftenreihe Stahlbau, RWTH Aachen, Germany, 2005.

[16] EN 1993-1-1. Eurocode 3: Design of steel strucutres / Part 1-1> General rules and rules for buildings. Brussels: European Committee for Standardization, 2011

[17] ANSYS, Inc. ANSYS® Academic Research, Release 15.0 [software]. Available from: http://www.ansys.com/

[18] EN 1863-1. Glass in building – Heat strengthened soda lime silicate glass – Part 1: Definition and description. Brussels: European Committee for Standardization.

[19] EN 12150-1. Glass in building – Thermally toughened soda lime silicate glass – Part 1: Definition and description. Brussels: European Committee for Standardization.

Ondřej Pešek was born in Vysoké Mýto, Czech Republic 23/10/1985. He finished master degree (title Ing.) in Structures and traffic constructions (field Design of Steel and Timber Structures) on Faculty of Civil Engineering, Brno University of Technology, Brno, Czech Republic in 2011, in 2011 he started his Ph.D. studies in field Design of glass structures at Brno University of Technology, Brno, Czech Republic.

He was WORKER at construction company, agriculture company and family farm. He also worked as CARTOGRAPHER for orienteering sport club. Actually he works as RESEARCHER at VFA PLUS company, Brno, Czech Republic (research in use of glass reinforced polymer material in traffic infrastructure) and as TUTOR at Department of Steel and Timber Structures, Faculty of Civil Engineering, Brno University of Technology, Brno, Czech Republic. He published more than twenty articles on problems of glass structures, one of them is Experimental verification of the actual behaviour of laminated glass element under out of plane loading (Napoli, Italy: European Convention for Constructional Steelwork, 2014). He is interest in stability problems of structural glass members.

Jindřich J. Melcher was born in Brno, Czech Republic 14/06/1939. He finished magister degree (title Ing.) in 1962 (Design of Steel and Timber Structures) at Brno University of Technology, Brno, Czech Republic. In 1969 he get a title CSc. (candidate of science), in 1977 Doc., in 1989 Prof. and in 1991 DrSc. (doctor of science). His field is design of steel structures and bridges, stability of steel members and experimental verification of load bearing members.

He worked as STATIC DESIGNER; in 1979 he was invited LECTURER at Lehigh University and Cornell University, USA. From 1985 to 1990 he was DEAN of Faculty of Civil Engineering, Brno University of Technology. From 1988 to 2005 he was HEAD of Institute of Metal and Timber Structures at the same university, actually he is HEAD of Testing Laboratory at Faculty of Civil Engineering, Brno University of Technology. He published approximately 300 conference papers and articles in journals and several textbooks. His researches are on design of steel structures including stability problems, probability approach, limit states, reliability and sustainability.

Prof. Melcher is member of ČKAIT (The Czech Chamber of Chartered Engineers and Technicians), technical committee for structural Eurocodes CEN/TC250/SC3, SSRC, IABSE and IIFC.